Journal of Agricultural Sciences (JAS) 32(3):669-681
DOI: 10.15832/ankutbd.1763304

J Agr Sci-Tarim Bili
e-ISSN: 2148-9297
jas.ankara.edu.tr

Nitrogen Estimation in Maize Using RGB Leaf Image Analysis and Deep Learning

Rabia Zafar[ab*], Muhammad Shahid Farid[a], Muhammad Hassan Khan[a], Rashid Mahmood[c]

[a]*Department of Computer Science, University of the Punjab, Lahore 54590, PAKISTAN*

[b]*Department of Computer Science and Engineering, University of Engineering and Technology, Narowal Campus, PAKISTAN*

[c]*Department of Soil Science, University of the Punjab, Lahore 54590, PAKISTAN*

ARTICLE INFO

Research Article
Corresponding Author: Rabia Zafar, E-mail: rabia.zafar@uet.edu.pk
Received: 12 August 2025 / Revised: 20 February 2026 / Accepted: 24 February 2026 / Online: 28 July 2026

Cite this article

Zafar R, Farid M S, Khan M H, Mahmood R (2026). Nitrogen Estimation in Maize Using RGB Leaf Image Analysis and Deep Learning. *Journal of Agricultural Sciences (Tarim Bilimleri Dergisi),* 32(3):669-681. DOI: 10.15832/ankutbd.1763304

ABSTRACT

The integration of digitization and automation into traditional farming has transformed agriculture, enhanced productivity and delivered significant economic benefits. Recent advances in deep learning (DL) provide new opportunities for automating crop monitoring and nutrient management. This paper proposes a framework for estimating nitrogen content in maize leaves using RGB images captured under field conditions. A UNet-based segmentation model isolates leaves from complex, uncontrolled backgrounds, and a convolutional neural network (CNN) extracts discriminative features. These features are evaluated using three regression models, Support Vector Regressor (SVR), Random Forest Regressor (RFR), and Gradient Boosting Regressor (GBR), to predict SPAD values, ranges from 24.9 to 59.5, an indirect measure of chlorophyll and nitrogen content. Experiments conducted on six maize varieties (three open-pollinated and three hybrid) across four growth stages yielded an overall lowest mean absolute error (MAE) of 3.56 and a correlation coefficient of 0.76. Aggregating results by dataset type, the best-performing method achieved an average MAE of 3.56 for OPV and 4.04 for Hybrid varieties. Further analysis by individual variety type revealed that RFR was most effective, attaining the lowest MAEs of 1.34 and 1.47 for OPV and Hybrid varieties, respectively. A second contribution is MaizeRGB, a comprehensive, publicly available dataset containing RGB images and ground-truth SPAD measurements for multiple maize varieties, nitrogen levels, and growth stages. The proposed approach demonstrates high accuracy, robustness to variable field conditions, and strong potential for low-cost, scalable nitrogen management in precision agriculture.

Keywords: Maize phenotyping, Precision agriculture, Neural Network, Image analysis, Machine Learning

1. Introduction

Smart and precision farming is an emerging paradigm in modern agriculture aimed at optimizing crop production through precise management of resources. By tailoring the application of seeds, water, fertilizers, and other inputs to the actual needs of plants, precision farming enables judicious resource utilization, thereby enhancing productivity, reducing production costs, and minimizing the environmental footprint of agriculture. This approach has gained global momentum due to its potential to address the twin challenges of feeding a growing population while maintaining ecological sustainability.

A considerable body of research has sought to equip farmers with empirical tools and decision-support systems for more efficient crop management. Notable examples include studies on disease classification (Özüpak et al. 2025; Alpsalaz et al. 2025), optimal fertilization strategies in enhancing plant nutrient uptake (Erman et al. 2025), assessments of soil fertility under different cultivation practices (Gürbüz & Kardeş 2024), and evaluations of nitrogen fixation capacity among various cultivars (Altuntaş et al. 2024). Among essential plant nutrients, nitrogen plays a central role in supporting vigorous vegetative growth, leaf development, and grain yield formation. Nitrogen deficiency can trigger a cascade of physiological constraints, including competition among plant organs for nitrogen translocation, delayed phenological development, reduced photosynthetic efficiency, and, ultimately, stunted growth and lower yield potential. Conversely, excessive nitrogen application poses equally severe challenges. Over-fertilization accelerates nitrogen losses from agricultural soils into the wider ecosystem, leading to eutrophication of water bodies, soil acidification, and increased emissions of nitrous oxide, a potent greenhouse gas (Li et al. 2024). These environmental and agronomic considerations underscore the critical need for precise, timely nitrogen estimation in crops to enable informed, site-specific fertilizer management (Ghazal et al. 2024; Haliloğlu & Aydogdu 2024). Traditionally, nitrogen content in plant tissue has been quantified using chemical and combustion-based laboratory methods such as the Kjeldahl (Richmond 1908) and Dumas (Sáez-Plaza et al. 2013) techniques. While these approaches remain accurate and widely recognized, they are inherently destructive, labour-intensive, time-consuming, and costly, making them unsuitable for large-scale or real-time field monitoring.

The introduction of non-destructive methods brought forward tools such as the SPAD chlorophyll meter, which estimates chlorophyll content, closely correlated with nitrogen levels, by measuring light absorbance in the red and infrared spectrum. Although SPAD meters provide rapid, in-situ readings without damaging plant tissue, their high cost and limitation to a small measurement area on the leaf restrict scalability (Adhikari et al. 2020). More advanced non-destructive approaches, including spectroscopy and spectral imaging (Lu et al. 2020; Colorado et al. 2020), rely on detecting subtle variations in leaf spectral signatures influenced by nitrogen compounds. From these measurements, indices such as the normalized vegetation index (NVI), normalized reflectance index (NRI), and green normalized vegetation index (GNVI) are derived to capture nitrogen-related changes in light reflectance and absorption. While these methods can be highly accurate, they require expensive sensors, produce large data volumes demanding substantial storage and computational capacity, and often require specialized expertise, factors that limit adoption in smallholder and resource-constrained farming systems.

In recent years, digital imaging has emerged as a more accessible and cost-effective alternative for nitrogen estimation. Readily available consumer-grade RGB cameras have been used to estimate nitrogen content at both the canopy and leaf levels. At the canopy scale, multi-resolution satellite imagery has been applied, although its effectiveness is often reduced by environmental interference (e.g., cloud cover, shadows), limited revisit times, and costs associated with high-resolution acquisitions (Pagola et al. 2009). At the leaf level, conventional cameras have been employed in various studies (Haider et al. 2021). Some studies also use DL models to get deep features from spectral data and passed to models to achieve better results e.g. (Wang et al. 2025; Li et al. 2024)**.** However, most of these works were conducted under controlled lighting and environmental conditions, limiting their applicability in real-world field scenarios characterized by variable illumination, complex backgrounds, and diverse growth stages. To address these challenges, the integration of machine learning (ML) and deep learning (DL) techniques into agricultural image analysis has shown considerable promise. DL methods, in particular, excel at learning complex, non-linear patterns from large datasets and can robustly extract meaningful features from noisy, heterogeneous field data.

In this study, an automated framework is proposed for precise in-field nitrogen estimation in maize that leverages ubiquitously available smartphone RGB imagery, eliminating the need for specialized hardware or software to bridge the technological accessibility gap for non-expert users identified by multiple studies such as (Gallegos et al. 2024).

The main contributions of this paper are:

- **Automated nitrogen estimation framework:** A computer-aided system for estimating nitrogen content in maize leaves from RGB images, requiring minimal human intervention limited to image capture.
- **Efficient segmentation model:** A deep learning model capable of automatically isolating maize plants and leaves at different growth stages, eliminating the need for manual selection of the region of interest.
- **Robust regression modelling:** A multi-model regression approach that uses features extracted from segmented leaf images to predict SPAD values, demonstrating consistent accuracy across different datasets.
- **Comprehensive public dataset:** A large-scale dataset comprising RGB images of maize crops at various growth stages, covering six varieties (three open-pollinated and three hybrid) and six nitrogen levels, paired with ground truth SPAD values. By releasing this dataset publicly, we aim to support future research and innovation in precision agriculture.

2. Material and Methods

2.1. Data acquisition

To bring out nitrogen level variations, an experiment on maize plants was conducted at Maize & Millet Research Institute, Yousafwala, Sahiwal, Pakistan (30.6854 N and 73.2052 E) in the Spring season of 2023, six maize cultivars including three F1 hybrids i.e. DK-9108, DK 6317, and DK-7024, and three open-pollinated varieties (OPV) i.e. Sahiwal Gold, Malka, and Gohar-19 were cultivated at six fertilizer nitrogen (N) levels. The N levels were calculated as multiples of the recommended dose of N (RDN; 220 kg/ha) i.e. 0, RDN/3, RDN/1.5, RDN, RDN×1.5, and RDN×3.

Table 1- Dataset collection date with actual and used counts for OPV and hybrid varieties datasets

Dataset Date	*OPV Actual*	*OPV Used*	*Hybrid Actual*	*Hybrid Used*
28/02/2023	323	314	284	268
18/03/2023	162	162	162	162
07/04/2023	162	160	130	130
28/04/2023	160	159	161	158



(a) (b) (c) (d)

Figure 1- Sample leaf images captured at different time periods, (a) leaf at 1 week after germination, (b) leaf at 5-6 leaves, (c) leaf at 8-10 leaves, (d) leaf at flowering

The experiment was conducted according to three times replicated Randomized Complete Block Design (RCBD) with maize cultivar and N application rate as experimental factors. Each Plot size was 50 m^2 where plant-to-plant and row-to-row distances were maintained as 25 cm and 75 cm, respectively. Whole fertilizers of phosphorus (P_2O_5) at 58 kg/ha and potassium (K_2O) at 90 kg/ha and one-fourth of N were applied as basal dose at the time of seedbed preparation, whereas the remaining N was equally divided into three splits and applied at 5-6 leaves, 8-10 leaves and at flowering. Each time of fertilizer application was followed by irrigation. Leaf images and SPAD values were obtained at four stages of the plant i.e. one week after germination, 5-6 leaves, 8-10 leaves, and flowering. To get the data middle part of the youngest fully expanded leaf was selected.

At each growth stage, data is collected, resulting in the generation of four distinct datasets, labeled as O1, O2, O3, and O4 for OPV, and H1, H2, H3, and H4 for hybrid varieties. These datasets allow us to assess the proposed system's performance at each stage of crop development, providing valuable insights into its functionality and effectiveness.

This dataset named 'MaizeRGB' will be publicly made available for research purposes at http://faculty.pucit.edu.pk/~farid/Research/MiazeRGB.html. Crop sample images were systematically taken within each plot. Consequently, we gathered these images from different smartphone cameras so that resolution and camera quality constraints can be taken into account. A brief description of the dataset is presented in Table 1 and visual leaf images captured at different times are shown in Fig. 1. The images were captured at resolution of 3120 × 4160 and downsized to 256 × 256 to optimize the efficiency of the ensuing image processing. This down-sampling balances computational efficiency for model training with the retention of gross visual features indicative of nitrogen status (e.g., overall chlorosis and interveinal discoloration). While fine leaf venation detail is reduced, this resolution is sufficient for capturing the primary color and texture patterns associated with nitrogen deficiency and is essential for enabling future real-time inference on mobile hardware. There is a difference between actual and used samples because during processing some sample's ground truth value was not recorded so those samples were discarded. The collected SPAD values, representing leaf chlorophyll content, exhibited a wide range from 24.9 to 59.5 across the entire dataset. For the OPV and Hybrid maize types, the ranges were 24.9–59.5 and 25.6–58.9, respectively.

2.2. Experimental design

The model generalization is evaluated by using a stratified random split, allocating 80% for training, 20% for testing. Processor Intel(R) Core(TM) i7-10510U CPU, installed RAM 8.00 GB, Storage 932 GB HDD , 238 GB SSD and 64-bit operating system are used for implementation.

2.3. Proposed methods

The proposed system is an ensemble method that uses DL and ML models for nitrogen content estimation in maize at multiple stages of growth. The framework consists of 3 major steps. The process begins with image segmentation from the background, achieved through a DL model. Next, features are extracted from the segmented images using advanced DL techniques. Finally, the nitrogen content is estimated through regression analysis based on the extracted features. Fig. 2 shows the block diagram of the proposed methodology.

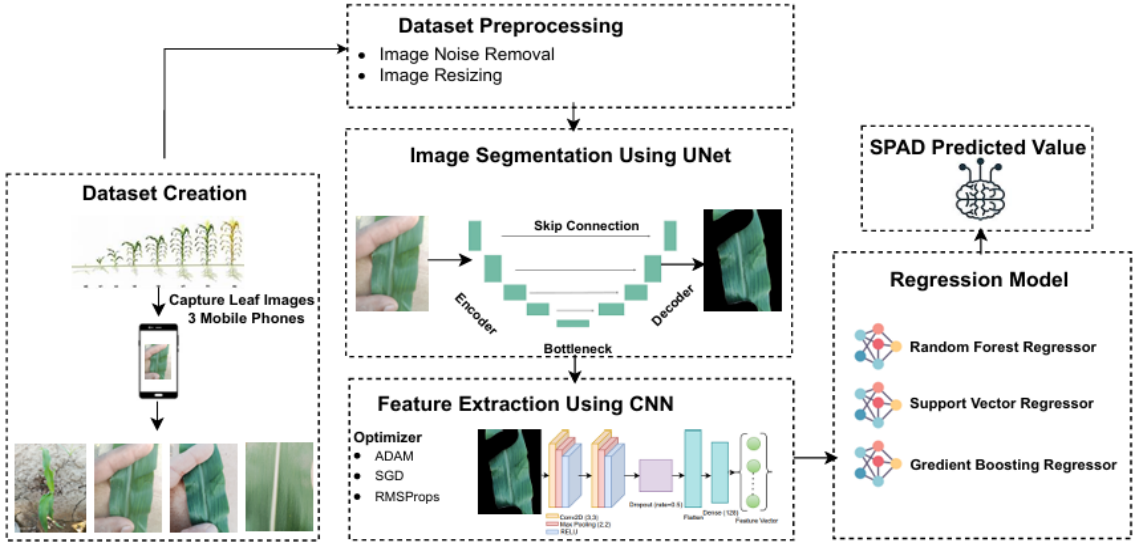


Figure 2- Comprehensive methodology adopted, encompassing data collection, preprocessing, leaf segmentation, regressor model training, and result evaluation

2.3.1. Leaf segmentation

Image segmentation serves as a fundamental step in extracting objects of concern. In prior research, images were captured under a controlled environment, in which background and interested region can be distinguished easily but in this study, the samples that are taken into account are not captured under a controlled environment. Images contain parts that are not important for estimating nitrogen e.g. soil, seeds, rocks, human body parts and shadows. So, to get accurate results the captured images were segmented to get a region of interest.

UNet (Ronneberger Olafand Fischer, 2015), a CNN is employed for segmentation as in (Özüpak et al. 2025) it is stated that this method achieves 98.97 % accuracy which is relatively high then other methods presented in literature. UNet is one of the DL models that use encoder-decoder architecture with skip connections which gives it the capability to retain detailed spatial information, extract regions of interest, and also minimize the loss of fine-grained spatial details during down-sampling and up-sampling processes. It encompasses the encoder block that progressively decreases spatial dimensions through convolutional layers, activation functions (ReLU) (Equation (1)) (Agarap, 2018) and batch normalization (Equation (2)) (Bjorck et al. 2018).

$$ReLU(x) = max(0, x) \tag{1}$$

$$\hat{x} = \frac{(x - \mu)}{\sqrt{\sigma^2 + \varepsilon}} \cdot \gamma + \beta \tag{2}$$

In Equation (2) (Bjorck et al. 2018), x is batch normalization layer's input, μ represents average, σ is the standard deviation of respective batch, γ is scale factor, β is shift parameter and ε represents small constant to avoid division by zero. It has a bottleneck layer that retains high-level features shown in Fig. 3. Whereas the decoder block upsampled the spatial dimensions using transposed convolutions and concatenates skip connections from the corresponding encoder stages. Multiple encoding and decoding stages were employed. The filter's quantity in each convolutional layer unfolds the capacity of the model to capture features of varying complexities. The UNet architecture culminates in a final convolutional layer with a sigmoid activation shown in Equation (3)(Hao et al. 2020), producing a binary segmentation mask as shown in the output layer.

$$Sigmoid(ws) = \frac{1}{(1 + e^{-ws})} \tag{3}$$

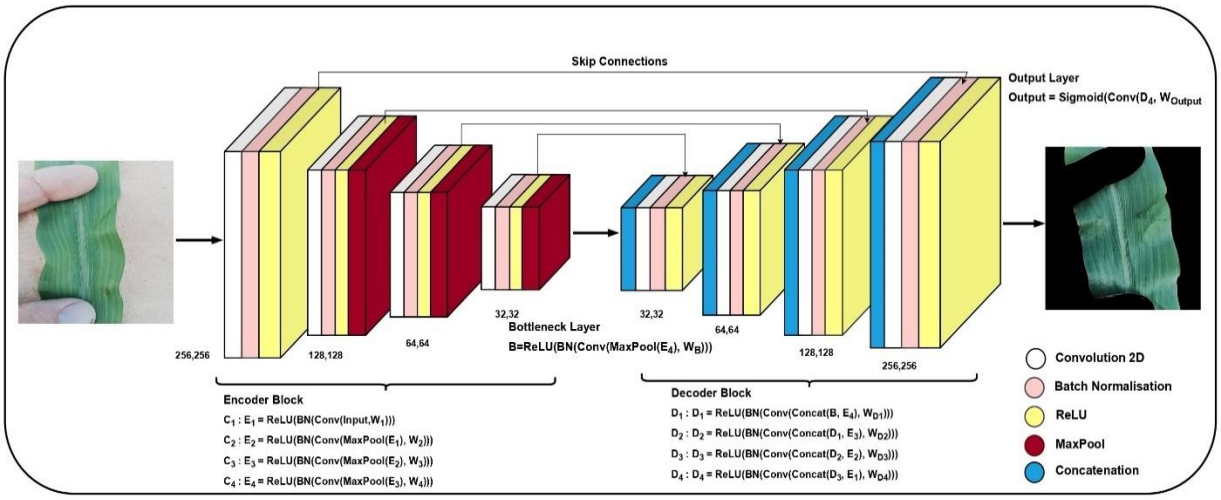


Figure 3- Architectural diagram of the UNet Model: illustrates the encoder-decoder structure, skip connections, and layer sizes for image segmentation

Fig. 3 shows the architecture of a simple encoder-decoder block of UNet model. In Equation(3) (Hao et al. 2020), ws is the weighted sum and e is the mathematical constant approximately equal to 2.71828. The generated masks are then used in training and validation steps to capture regions of interest. The W_i terms depicted the weight matrices linked with the corresponding convolutional layers. The hyper-parameters that are used in UNet architecture are shown in Table 2. Fig. 4 presents the segmentation results of the images shown in Fig. 1 respectively. It is worth noting how accurately the leaves are segmented from the different backgrounds at various growth stages.

Table 2- Summary of hyperparameters used for the UNet model

Hyperparameter/Detail	***Value***
Batch Size	8
Learning Rate	1×10^{-4}
Epochs	20
Height	256
Width	256
Activation Functions	ReLU
Final Activation Function	Sigmoid

2.3.2. Feature extraction

The process of Feature extraction is to mine meaningful and discriminative information from raw data. Concerning images, CV and traditional ML demand domain expertise to design and engineer handcrafted features. Conversely, DL models are capable of learning and extracting hierarchical features from unprocessed data, obsoleting the need for hand crafted feature engineering.



(a) (b) (c) (d)

Figure 4- The segmentation results of the images shown in Fig 1, respectively

In this study, a CNN model, shown in Fig. 5, is used to extract features by omitting the final regression or classification layer. CNN is a type of DL model designed specifically for images that perform convolutions over input images to generate feature

maps. These feature maps contain patterns and structures in the input. The size reduction of feature maps is done by pooling layers that perform down-sampling. In this research, max-pooling is used. Later on, non-linearity is introduced by ReLU to learn complex patterns from data. During training, the architecture adjusts its weights to lessen the difference between predicted and ground truths, gradually improving its ability to extract meaningful features. The hyperparameters used for the proposed CNN architecture are given in Table 3.

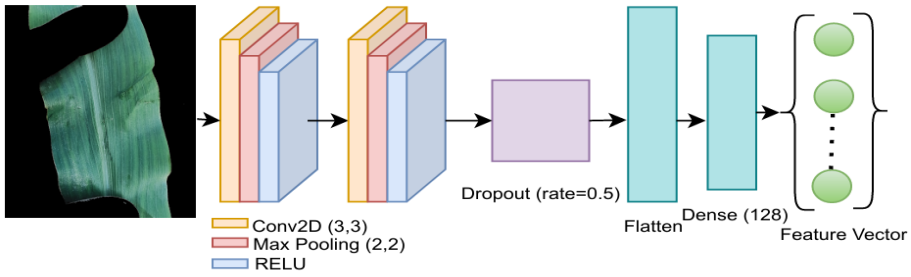


Figure 5- Architectural diagram of the CNN for feature extraction

2.3.3. Regression analysis

After the feature extraction phase, the features are given as input to the regression algorithms to estimate nitrogen content for input data. For regression, SVR, RFR, and GBR are used to get better insights. RFR (Segal, 2004) is an ensemble learning algorithm that captures the outputs of decision trees to produce a robust and accurate model. Deep inside, it recursively splits the dataset to create a set of rules based on a distinct subset of the training data to predict the target variable. The final result is computed by averaging predictions of trees shown in Equation (4) (Segal, 2004).

$$\hat{y}_{RF}(I) = \frac{1}{N}\sum_{i=1}^{N} h_i(I) \tag{4}$$

Table 3- CNN model hyperparameters

Layer	***Hyperparameters***
Convolutional	Depth: 32 Window Size: (3,3) Activation: ReLU Input Dimension: (224, 224, 3)
Max Pooling	Pool Size: (2, 2)
Convolutional	Depth: 64, Window Size: (3, 3) Transfer function: ReLU
Max Pooling	Pool Size: (2, 2)
Regularization	Rate: 0.5
Dense	Units: 128 Transfer function: ReLU
Optimizer	Adam, Stochastic Gradient Descent (SGD) , Root Mean Squared Propagation (RMSProps)

Where N is the count of trees and $h_i(I)$ is the respective prediction of a tree. GBR (Prettenhofer & Louppe 2014) is also an ensemble method that also involves trees as predictors. Irrespective of the same baseline RFR and GBR have a certain difference in processing that GBR sequentially corrects the error of the previous tree to get a better estimate.

$$\hat{y}_{GBR}(I) = \frac{1}{N}\sum_{i=1}^{N} \alpha_i h_i(I) \tag{5}$$

Equation (5) (Prettenhofer & Louppe 2014) shows the mathematical representation of GBR, i.e. I is input, $h_i(I)$ is a prediction of i^{th} tree and α_i is the weight of each tree. The third regressor that is used is SVR (Awad et al. 2015) which is a type of support vector machine. It finds a hyperplane that best explains the relationship of input and output using a kernel function, Equation (6) (Awad et al. 2015) depicts the working of SVR where α_i and α_i^* are Lagrange multipliers, R is Radial Basis function and b is a bias.

$$\hat{y}_{SVR}(I) = \sum_{i=1}^{N}(\alpha_i - \alpha_i^*)\ R(I, I_i) + b \tag{6}$$

These three best regressors have been investigated to find the best-suited for maize crop. The parameters settings of each regressor used in experiments are listed in Table 4. A large number of experimental evaluations are executed to assess the proposed method, explained in the following section.

Table 4- Summary of hyperparameters used for the regressors

Regressor	Hyperparameters
RFR (Random Forest Regressor)	n_estimators = 100
GBR (Gradient Boosting Regressor)	n_estimators = 100
SVR (Support Vector Regressor)	Kernel = RBF Regularization factor = 1.0

3. Results and Discussion

The primary objective of this research was to develop an affordable, user-friendly, and accurate system for nitrogen estimation, enabling farmers to regulate fertiliser application and other agronomic parameters more effectively. SPAD readings were adopted as the ground truth reference because SPAD meters measure chlorophyll content, which is strongly correlated with nitrogen levels, but not perfectly equivalent to, leaf nitrogen status. Furthermore, readings can vary across the leaf surface. To minimize this variability and align with the image field of view, we adopted a standardized protocol, three SPAD measurements were taken from the middle third of each target leaf, avoiding the midrib, and averaged to produce a single value per leaf image. This protocol aimed to ensure that the ground truth data corresponded as closely as possible to the leaf tissue captured in the photograph.

Although SPAD meters offer high accuracy, their high cost and requirement for skilled operation underscore the need for an accessible, automated alternative that can be deployed widely.

To evaluate the proposed framework, multiple experiments were conducted across varying crop categories, types, and growth stages to address limitation in plant phenotyping tasks (Alpsalaz et al. 2025). Two maize categories, Hybrid (H) and OPV (O), were cultivated, each comprising three distinct types (T1, T2, T3). Data were collected at four crop growth stages for each type, resulting in a comprehensive dataset covering the full growth cycle from cultivation to harvest. The total number of datasets was computed as:

$$N_{Ds} = B \times T \times S \tag{7}$$

Where: B, number of categories (2); T, number of types per category (3); S, number of growth stages (4)

This yields $N_{Ds}=2\times3\times4=24$ datasets in total.

In the dataset notation, the two maize categories are represented as O (OPV) and H (Hybrid). The four growth stages are denoted by numbers 1–4, so, for example, O1 corresponds to the OPV dataset at stage 1, and H4 corresponds to the Hybrid dataset at stage 4. Within each category, the three types are labelled T1, T2, and T3.

The initial experiments were conducted by applying the proposed methodology to different growth stages, without distinguishing between the types within each category. The aggregated results are presented in Table 5 for the Hybrid category and Table 6 for the OPV category.

To further assess the robustness and applicability of the proposed framework, validation was also performed on each type individually within both crop categories. This allowed for evaluation of model performance across genetic variations and growth characteristics, providing deeper insight into the adaptability of the method for diverse maize varieties.

Table 5- Comprehensive performance evaluation of optimization algorithms on regression models across multiple hybrid category of maize datasets

Dataset	*ADAM*			*SGD*			*RMSProps*		
	RFR	*SVR*	*GBR*	*RFR*	*SVR*	*GBR*	*RFR*	*SVR*	*GBR*
H1	3.9909	3.8767	4.4873	4.2568	3.8613	4.1035	3.9481	3.8690	4.2430
H2	3.4306	3.4933	3.3029	3.8172	3.7168	3.6862	3.7252	3.7452	4.1800
H3	3.7221	4.1813	4.0576	4.2836	4.2547	4.6468	3.9947	4.2477	3.7417
H4	5.0242	5.3574	4.7499	4.7903	5.5419	4.4426	5.3520	5.4415	5.1724

Table 6- Comprehensive performance evaluation of optimization algorithms on regression models across multiple OPV category of maize datasets

Dataset	*ADAM*			*SGD*			*RMSProps*		
	RFR	*SVR*	*GBR*	*RFR*	*SVR*	*GBR*	*RFR*	*SVR*	*GBR*
O1	2.6890	2.6280	2.7789	2.5884	2.6495	2.7490	2.5497	2.5889	2.6396
O2	4.6885	4.5822	4.5733	4.0798	4.2102	4.3152	4.6081	4.5816	4.9762
O3	1.7433	3.6113	2.2102	2.1629	3.5114	2.3193	1.9189	3.7131	2.6344
O4	6.3912	6.4094	6.4312	5.4372	6.0391	5.2631	5.4106	6.1159	5.3125

For dataset O1, the best method is SGD optimizer with RFR, which achieved the lowest mean absolute error (MAE) of 2.5884. For dataset O2, the same method, SGD and RFR, also performed the best with an MAE of 4.0798, indicating consistent superiority in these datasets. In the case of dataset O3, ADAM optimization algorithm combined with RFR was the most effective, with the lowest MAE of 1.7433. Finally, for dataset O4, the SGD optimization algorithm combined with GBR demonstrated the best performance, achieving an MAE of 5.2631. These results suggest that SGD and RFR are generally effective across multiple datasets. Similarly, for dataset H1, the best method is RMSProps with RFR, which achieved the lowest MAE of 3.9481.

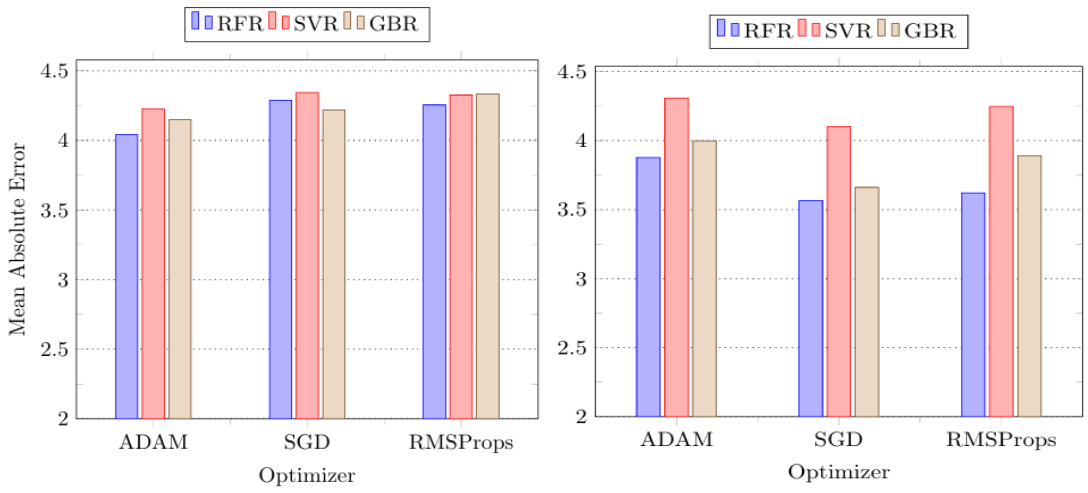


Figure 6- Performance of the three regressors with different optimizers on Hybrid (a), and OPV (b) datasets

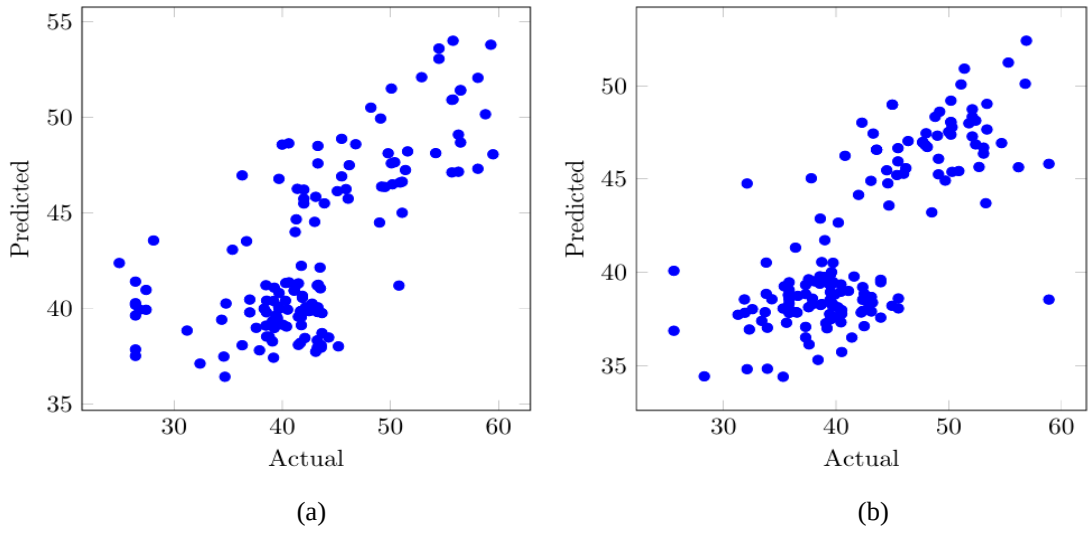


Figure 7- Relationship between actual and predicted values for OPV and Hybrid dataset. (a) Actual vs Predicted for hybrid maize crops, (b) Actual vs Predicted for OPV maize crops

For dataset H2, ADAM optimization algorithm combined with GBR was the most effective, with the lowest MAE of 3.3029. In the case of dataset H3, ADAM optimization algorithm combined with RFR demonstrated the best performance, achieving an

MAE of 3.7221. Finally, for dataset H4, the SVD optimization algorithm combined with GBR performed the best, with an MAE of 4.4426. Here we observe that for hybrid GBR performs well but each time with a different optimizer. Hence there is no consistent performing optimizer and regressor for hybrid. But if a general method is needed to be considered for each dataset, it appears for OPV, SGD with RFR has the lowest average MAE (3.56707), indicating the best overall performance across all four datasets, and for Hybrid, ADAM with RFR has the lowest average MAE (4.04195). Overall, OPV datasets are easier to model than hybrids, averaging the best method per dataset yields 3.41 MAE for OPV versus 3.83 for hybrids. Tree ensembles dominate the leaderboard, RFR is the most frequent winner (H3, O1, O2, O3) and remains competitive elsewhere, Across optimizers, no single choice is universally best: SGD is the most consistently strong (wins H1, H4, O2, O4).

From Fig. 6, we can observe that the distribution of MAE values varies with both the regression algorithm and the optimizer used. This kind of visualization is invaluable for identifying which combinations of algorithms and optimizers yield the most accurate and consistent predictions for all stages of the crop. It is found that data at different stages impact the model training and it is very difficult to get a single precise model for nitrogen estimation at all stages of the crop.

Secondly, the proposed method is employed on the dataset by considering each variety at different stages of the crop. The experimental outcomes are presented in Tables 7 and 8.

Considering types of OPV, RFR performs well for both T1 and T2 with MAEs of 1.34 and 1.84 respectively whereas SVR gives better results having MAE of 2.02 for T3. For hybrid, RFR outperforms for T1 and T3 with MAEs of 1.47 and 3.79 respectively, while GBR gives better results for T2 with an MAE of 2.65. The scatter plots presented in Fig 7 exhibit a fairly linear trend, suggesting a strong correlation between the real and predicted values i.e. correlation coefficient value 0.76 and 0.71 for OPV and Hybrid, respectively.

Fig. 7 illustrates a sample transaction within our proposed system. A leaf image from O3 dataset is tested from segmentation to prediction. The results reveal a minimal discrepancy of merely 0.04 between the true and the predicted values. Additionally, it is evident that human intervention is significantly limited, with only the necessity of capturing an image, the remaining processes are conducted automatically. The outcome of proposed methodology fairly depicts that in comparison to previous approaches it gives valuable insights regarding prediction of SPAD at various stages of multiple breeds and types and also it is not labor intensive, requires no specialized expertise, and is cost-effective.

Table 7- Comprehensive performance evaluation of optimization algorithms on regression models across multiple types of OPV category of crop datasets

Dataset		***ADAM***			***SGD***			***RMSProps***		
Category	Type	RFR	SVR	GBR	RFR	SVR	GBR	RFR	SVR	GBR
O1	T1	2.2906	2.0889	2.1592	2.2102	2.0977	2.0868	2.1705	2.1538	2.3176
O1	T2	3.2907	3.1744	3.3997	3.1709	3.2867	3.5332	3.1461	3.1371	3.1809
O1	T3	2.1692	2.3054	2.4186	2.079	2.2088	2.1921	2.0214	2.1501	2.1415
O2	T1	4.0872	4.4216	4.1162	3.4279	3.623	3.943	4.7025	4.0556	5.3446
O2	T2	3.839	3.2573	3.6273	3.2866	3.1871	3.2193	3.2683	3.6252	3.6872
O2	T3	6.3093	6.3325	6.1656	5.6835	6.0251	6.0024	6.1215	6.2551	6.1544
O3	T1	1.3478	3.0998	2.3269	1.8018	3.0982	1.9153	1.7673	3.5467	2.4537
O3	T2	1.8499	4.0033	1.9018	2.175	3.9938	2.4975	1.8599	3.7113	2.7441
O3	T3	2.1402	3.8141	2.4317	2.6295	3.4729	2.6401	2.1932	3.9372	2.7413
O4	T1	4.4455	5.1996	5.926	4.0483	4.905	3.5607	4.0024	5.4646	4.8275
O4	T2	7.9885	7.8294	7.3942	6.6051	7.292	6.6945	6.9688	7.2767	6.7874
O4	T3	5.6358	5.2758	5.3824	4.8551	5.0983	4.5496	4.2384	4.889	3.4494

Table 8- Comprehensive performance evaluation of optimization algorithms on regression models across multiple types of hybrid category of crop datasets

Dataset		***ADAM***			***SGD***			***RMSProps***		
Category	Type	RFR	SVR	GBR	RFR	SVR	GBR	RFR	SVR	GBR
H1	T1	1.4708	1.8886	2.2331	2.1311	1.9028	2.1116	1.6591	1.7632	1.7548
H1	T2	3.7769	3.0601	4.2394	3.8531	3.0588	3.6008	3.6391	3.0925	3.8626
H1	T3	6.3309	6.5226	6.6499	6.5062	6.4656	6.3649	6.2148	6.5624	6.7621
H2	T1	1.7934	1.6885	1.9836	3.0587	1.6752	2.887	2.5537	1.5412	2.2137
H2	T2	3.0521	2.7454	2.7916	3.1228	2.8927	2.6597	3.7759	3.0622	4.6259
H2	T3	4.8163	5.2098	4.5375	4.7557	5.6461	4.8436	4.533	5.7097	5.3296
H3	T1	3.1443	2.6585	3.8168	4.2036	3.0985	5.0669	3.0118	2.8216	2.9159
H3	T2	4.1369	5.5391	4.4245	4.543	5.6611	4.8214	5.6547	5.9755	4.8123
H3	T3	4.0415	4.8172	4.0399	4.171	4.4454	4.0444	3.7958	4.4885	3.8264
H4	T1	4.8423	4.6246	4.7052	5.5326	5.1124	4.7155	5.566	5.0732	4.5844
H4	T2	4.9458	5.8338	4.8772	4.8023	6.0639	4.2559	5.4395	5.882	5.9434
H4	T3	5.2609	5.5904	4.6747	4.1046	5.4578	4.3643	5.0781	5.3759	5.006

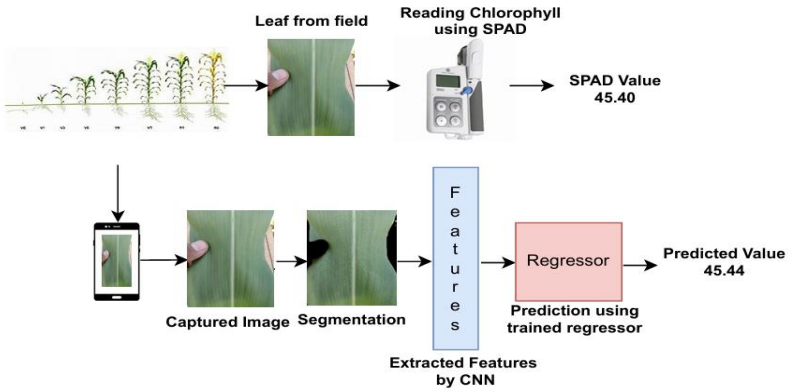


Figure 8- Complete sample run of the proposed method: the entire workflow from data input and preprocessing to output generation

3.1. Comparison with other architectures

The comparative performance of the pretrained architectures shown in Table 9 further underscores the efficacy of CNN framework. While the Vision Transformer model showed competitive results, CNN achieved a MAE 3.41 and 3.83 for OPV and hybrids respectively under per dataset selection, and 3.56 MAE for OPV and 4.04 for hybrids under a single fixed configuration, outperforming Vit and substantially surpassing larger convolutional networks like ResNet50 and VGG16. Notably, this superior accuracy is achieved with a model that is architecturally simpler and has a lower feature dimension than the pretrained counterparts. This indicates that CNN avoids the overfitting and redundancy common in generic, large-scale networks when applied to specialized agricultural vision tasks, providing an optimal balance of accuracy and efficiency for field deployment, it also shows depth-accuracy paradox depicting that deeper network are not always suitable for every task. Beyond predictive accuracy, the architectural efficiency of CNN offers significant practical advantages for field deployment.

Table 9- Comparison of test set MAE for nitrogen estimation across different model architectures

Model	***MAE (OPV)***	***MAE (Hybrid)***
Vision Transformer (ViT)	3.78	4.72
VGG16	4.04	4.88
EfficientNet	4.05	4.98
ResNet50	4.01	5.33
Proposed (per dataset selection)	**3.41**	**3.83**
Proposed (Fixed Configuration)	**3.56**	**4.04**

This model operates with a substantially lower feature dimension than the high-dimensional representations of pre-trained networks like ResNet50 (2048), EfficientNet (1280), or ViT (768). This reduced complexity translates directly to a smaller memory footprint, lower computational demand, and faster inference times. Consequently, the model is inherently more suitable for integration into real-time, on-device applications on smartphones or edge computing platforms, enabling scalable nitrogen estimation without reliance on cloud connectivity or high-end processing hardware.

3.2. Comparison with existing methodology

The model robustness is tested by using multiple mobile phone models, across different times of day, lighting conditions, field sites and varieties. This introduces significant variation in image quality, color response, and scene geometry, simulating a real-world deployment scenario in contrast to studies that use special image capturing equipment and setups such as in (Haider et al. 2021; Sun et al. 2024). A key advantage is the fully automated workflow after image capturing, which uses a U-Net for leaf segmentation to eliminate the need for controlled backgrounds, fixed lighting, or manual cropping. This addresses a major limitation in many RGB, UAV, and SPAD-based methods. While hyperspectral and multispectral systems can capture detailed spectral information (Wang et al. 2025), they face challenges like data redundancy, high cost, and sensitivity to acquisition conditions, often requiring complex preprocessing that can introduce noise (Candiani et al. 2022).

In contrast, our CNN-based framework demonstrated robust performance by achieving a mean absolute error (MAE) of 3.56 and a correlation coefficient of 0.76. This result is significant as it was achieved on a test set comprising images from previously unseen phone models and field locations, indicating successful generalization across domains. For OPV maize types, MAE

values across regression models ranged from 1.34 to 2.02, while for Hybrid types, MAE values ranged from 1.47 to 3.79. Notably, this performance is competitive with established spectral and modeling techniques. Proposed method's correlation coefficient R = 0.76, compares favorably with results from advanced models such as Vision Transformers presented in (Ghazal et al. 2024) that achieve 0.69 accuracy and traditional statistical approaches including PLSR, which achieved $R^2 = 0.72$ (Siqueira et al. 2022), and method presented by (Xin et al. 2024) that achieve R^2=0.75. It also aligns with results from study utilizing custom vegetation indices (Vesali et al. 2015) having R^2=0.72.

Similar to the work of Sun et.al (Sun et al. 2024), our method bypasses the need for handcrafted vegetation indices or spectral transformations, streamlining both model development and field application. However, the added robustness provided by automated segmentation and field-condition training allows our RGB-based solution to rival, and in some cases exceed, the performance of more complex UAV-based or hyperspectral systems. This establishes our framework as a scalable, low-cost, and field-ready tool for real-time nitrogen estimation in maize.

4. Conclusions

The SPAD value is a widely adopted metric in agriculture for estimating chlorophyll content in plant leaves, and, given the strong relationship between chlorophyll concentration and nitrogen availability, it serves as a reliable indirect indicator of plant nitrogen status. In this work, we introduced a comprehensive dataset of maize crop images captured at multiple growth stages using RGB cameras, accompanied by ground-truth SPAD measurements. Leveraging this dataset, we proposed a novel nitrogen estimation framework that integrates a UNet-based deep learning model for automated leaf segmentation and a CNN-based feature extractor, followed by regression modelling to predict SPAD values. The CNN model was evaluated across different optimizer functions, growth stages, and crop types, with extracted features subsequently used to train multiple regressors. Among the models tested, the RFR consistently achieved the highest predictive accuracy in both experimental setups with value 4.04 for Hybrid and 3.56 for OPV. This demonstrates the potential of combining DL-based image processing with ensemble regression for robust, non-destructive nitrogen estimation under real-world field conditions. The proposed approach offers distinct practical utility, it is cost-efficient, scalable, and designed with accessibility in mind, enabling farmers, particularly in resource-limited settings, to perform nitrogen estimation directly via consumer-grade smartphones. By supporting more precise fertilizer application, this method contributes to improved crop productivity, reduced input costs, and minimized environmental impact.

The model generalizes well across the tested field conditions and varieties, its performance in radically different agro-climatic zones or under extreme abiotic stress requires further validation. Future work will focus on addressing current limitations related to dataset size and diversity, expanding the approach to other crops, and exploring additional deep learning and hybrid spectral-RGB architectures to further improve estimation accuracy. These advancements aim to strengthen the applicability and generalizability of the framework, ultimately promoting sustainable, technology-enabled agricultural practices.

Acknowledgments

The authors would like to thank Dr. Amjad Khan, Senior Scientist at Maize & Millets Research Institute, Yusafwala, Sahiwal and Dr. Muhammad Faisal, Assistant Professor (then) at Department of Soil Science, University of the Punjab, Lahore for their assistance in data collection.

Author Declarations

Authors' contributions: Conceptualization: M.S.F., R.Z., Methodology: M.S.F., R.Z., M.H.K. Software: M.S.F., R.Z., M.H.K., Writing---original draft preparation: M.S.F., R.Z., writing---review and editing: M.S.F., R.Z., R.M., supervision: M.S.F., R.M., M.H.K., Project administration: M.S.F., R.Z., M.H.K., Funding acquisition: M.S.F., R.M., validation, formal analysis, investigation, resources, and data curation: M.S.F., R.Z., M.H.K., R.M.

Conflict of interest/Competing interests: The author(s) declare no conflict of interest.

Ethics approval/declarations: No need/ Not applicable.

Data Declaration Statement: The dataset named 'MaizeRGB' will be publicly made available for research purposes at http://faculty.pucit.edu.pk/~farid/Research/MaizeRGB.html

Funding: This research was partially supported by a research grant (No. 21-140) from Punjab Agricultural Research Board (PARB), Pakistan.

Consent to participate: Not applicable.

Consent for publication: Not applicable.

Data availability: Data is available online.

References

Adhikari R, Li C, Kalbaugh K & Nemali K (2020). A low-cost smartphone controlled sensor based on image analysis for estimating whole-plant tissue nitrogen (N) content in floriculture crops. *Computers and Electronics in Agriculture* 169: 105173. https://doi.org/10.1016/j.compag.2019.105173

Agarap A F (2018). Deep learning using rectified linear units (relu). ArXiv Preprint ArXiv:1803.08375. https://doi.org/10.48550/arXiv.1803.08375

Alpsalaz F, Özüpak Y, Aslan E & Uzel H (2025). Classification of maize leaf diseases with deep learning: Performance evaluation of the proposed model and use of explicable artificial intelligence. Chemometrics and Intelligent Laboratory Systems 105412. https://doi.org/10.1016/j.chemolab.2025.105412

Altuntaş Y, Elkoca E, & Kodaz S (2024). Impact of Mesorhizobium ciceri Inoculation on Symbiotic Nitrogen Fixation of Various Chickpea (Cicer arietinum L.) Cultivars. *Journal of Agricultural Production* 5(4): 255–264. https://doi.org/10.56430/japro.1565531

Awad M, Khanna R, Awad M & Khanna R (2015). Support vector regression. *Efficient Learning Machines: Theories, Concepts, and Applications for Engineers and System Designers* pp. 67–80

Bjorck N, Gomes C P, Selman B & Weinberger K Q (2018). Understanding batch normalization. *Advances in Neural Information Processing Systems 31*

Candiani G, Tagliabue G, Panigada C, Verrelst J, Picchi V, Rivera Caicedo J P & Boschetti M (2022). Evaluation of hybrid models to estimate chlorophyll and nitrogen content of maize crops in the framework of the future CHIME mission. *Remote Sensing* 14(8): 1792. https://doi.org/10.3390/rs14081792

Colorado J D, Cera-Bornacelli N, Caldas J S, Petro E, Rebolledo M C, Cuellar D & others (2020). Estimation of nitrogen in rice crops from UAV-captured images. *Remote Sens* 12: *3396.* https://doi.org/10.3390/rs12203396

Erman M, Çğ F& Ceritoğlu M (2025). Optimizing Fenugreek (Trigonella foenum-graecum L.) Cultivation: Role of Rhizobium Inoculation and Phosphorus Fertilization on Growth, Nodulation, and Yield Attributes. *Turkish Journal of Applied Sciences and Technology* 6(1): 43–53. https://doi.org/10.70562/tubid.1662619

Gallegos Á, Gavito M E & Ferreira Medina H (2024). Foliar Nitrogen Estimation with Artificial Intelligence and Technological Tools: State of the Art and Future Challenges. *International Journal of Advanced Computer Science & Applications* 15(6)

Ghazal S, Kommineni N & Munir A (2024). Comparative analysis of machine learning techniques using RGB imaging for nitrogen stress detection in maize. *AI* 5(3): 1286. https://doi.org/10.3390/ai5030062

Ghazal S, Munir A & Qureshi W S (2024). Computer vision in smart agriculture and precision farming: Techniques and applications. *Artificial Intelligence in Agriculture.* https://doi.org/10.1016/j.aiia.2024.06.004

Gürbüz M A & Kardeş T A (2024). Sunflower-nitrogen calibration based on the amount of mineral nitrogen in soil under rainfed conditions in thrace region. *Soil Studies* 13(1): 43–54. https://doi.org/10.21657/soilst.1520597

Haider T, Farid M S, Mahmood R, Ilyas A, Khan M H, Haider S T A, Chaudhry M H & Gul, M. (2021). A Computer-Vision-Based Approach for Nitrogen Content Estimation in Plant Leaves. *Agriculture* 11(8). https://doi.org/10.3390/agriculture11080766

Haliloğlu H & Aydogdu A (2024). The effect of different nitrogen doses on growth attributes of some sunflower (Helianthus annuus L.) cultivars grown as second crop. *Akademik Ziraat Dergisi 13*(1): 129–136. https://doi.org/10.29278/azd.1393338

Hao W, Yizhou W, Yaqin L & Zhili S (2020). The role of activation function in CNN. *2020 2nd International Conference on Information Technology and Computer Application (ITCA)* 429–432. 10.1109/ITCA52113.2020.00096

Li J, Ge Y, Puntel L A, Heeren D M, Bai G, Balboa G R, Gamon J A, Arkebauer T J & Shi Y (2024). Integrating UAV hyperspectral data and radiative transfer model simulation to quantitatively estimate maize leaf and canopy nitrogen content. *International Journal of Applied Earth Observation and Geoinformation* 129: 103817. https://doi.org/10.1016/j.jag.2024.103817

Li Z W, Wang G Y, Khan K, Yang L, Chi Y X, Wang Y & Zhou X B (2024). Irrigation combines with nitrogen application to optimize soil carbon and nitrogen, increase maize yield, and nitrogen use efficiency. *Plant and Soil* 499(1): 605–620. https://doi.org/10.1007/s11104-024-06480-6

Lu B, Dao P D, Liu J, He Y & Shang J (2020). Recent advances of hyperspectral imaging technology and applications in agriculture. *Remote Sensing* 12(16): 2659. https://doi.org/10.3390/rs12162659

Özüpak Y, Alpsalaz F, Aslan E & Uzel H (2025). Hybrid deep learning model for maize leaf disease classification with explainable AI. *New Zealand Journal of Crop and Horticultural Science* 1–23. https://doi.org/10.1080/01140671.2025.2519570

Pagola M, Ortiz R, Irigoyen I, Bustince H, Barrenechea E, Aparicio-Tejo P, Lamsfus C & Lasa B (2009). New method to assess barley nitrogen nutrition status based on image colour analysis: Comparison with SPAD-502. *Computers and Electronics in Agriculture* 65(2): 213–218. https://doi.org/10.1016/j.compag.2008.10.003

Prettenhofer P & Louppe G (2014). Gradient boosted regression trees in scikit-learn. *PyData 2014*

Richmond H D (1908). The estimation of nitrogen. *Analyst* 33(386): 179–184

Ronneberger O, Fischer P & Brox T (2015). U-Net: Convolutional Networks for Biomedical Image Segmentation. *International conference on Medical Image Computing and Computer-Assisted Intervention – MICCAI* 234–241. https://doi.org/10.1007/978-3-319-24574-4_28

Sáez-Plaza P, Michałowski T, Navas M J, Asuero A G, & Wybraniec S (2013). An overview of the Kjeldahl method of nitrogen determination. Part I. Early history, chemistry of the procedure, and titrimetric finish. *Critical Reviews in Analytical Chemistry* 43(4): 178–223. https://doi.org/10.1080/10408347.2012.751786

Segal M R (2004). Machine learning benchmarks and random forest regression. *UCSF: Center for Bioinformatics and Molecular Biostatistics*

Siqueira R, Mandal D, Longchamps L & Khosla R (2022). Assessing nitrogen variability at early stages of maize using mobile fluorescence sensing. *Remote Sensing* 14(20): 5077. https://doi.org/10.3390/rs14205077

Sun L, Yang C, Wang J, Cui X, Suo X, Fan X, Ji P, Gao L & Zhang Y (2024). Automatic Modeling Prediction Method of Nitrogen Content in Maize Leaves Based on Machine Vision and CNN. *Agronomy* 14(1). https://doi.org/10.3390/agronomy14010124

Sun X, Zhang P & Wang Z (2024). Potential of multi-seasonal vegetation indices to predict rice yield from UAV multispectral observations. *Precision Agriculture* 1–27. https://doi.org/10.1007/s11119-023-10109-6

Vesali F, Omid M, Kaleita A & Mobli H (2015). Development of an android app to estimate chlorophyll content of corn leaves based on contact imaging. *Computers and Electronics in Agriculture* 116: 211–220. https://doi.org/10.1016/j.compag.2015.06.012

Wang D, Struik P C, Liang L & Yin X (2025). Estimating leaf and canopy nitrogen contents in major field crops across the growing season from hyperspectral images using nonparametric regression. *Computers and Electronics in Agriculture* 233: 110147. https://doi.org/10.1016/j.compag.2025.110147

Xin Q I, Yang W, YouLiang Y E, YuLong G U O, YaNan Z & others (2024). Nitrogen Nutrition Diagnosis Method Based on Mobile Phone Image of Summer Maize Canopy. *Scientia Agricultura Sinica* 57(20): 4094–4106. https://doi.org/10.3864/j.issn.0578-1752.2024.20.014



Copyright © 2026 The Author(s). This is an open-access article published by Faculty of Agriculture, Ankara University under the terms of the Creative Commons Attribution License which permits unrestricted use, distribution, and reproduction in any medium or format, provided the original work is properly cited.